ISSN: 0974-5823 Vol. 7 No. 1 January, 2022

International Journal of Mechanical Engineering

A 3D CFD simulation of cavitation phenomena for a centrifugal pump with multi rotational speed and pressure

Hasan Shakir Majdi
Department of Chemical Engineering & Petroleum Industries, Al-Mustaqbal University College, Hillah, Babil, Iraq,

Laith Jaafer Habeeb
Training & Workshop Center, University of Technology – Iraq, Baghdad, Iraq

Jinan Mahdi Hadi
Mechanical Engineering Department, University of Technology – Iraq, Baghdad, Iraq

Dragoljub Zivkovic
University of Nis, Nis, Serbia

Abstract

With the progress of development in the design of centrifugal pumps, it has become necessary to solve the problems that occur to these pumps. And the most important of these problems is the phenomenon of cavitation that occurs as a result of the increase in pressure of the fluids transmitted as a result of the rotation of the centrifugal pump. And due to this pressure, the fluid turns into steam that reduces the pump's resistance on the one hand. In this research paper, the effect of the pressure entering the pump & the speed of rotation of the centrifugal pump was studied to find out which pressures can be controlled in order not to get cavitation & reduce this phenomenon. Where a group of high pressures (1 bar to 5 bar) was used with a difference of 1 bar for each case & also a difference for the rotational speed used, where three rotational speeds (800, 1000 & 1200) rpm were used. It has been proven through the extracted results of the velocity of the fluid, which is the water, & the amount of vapor produced by the cavitation phenomenon that with the pressure rise the fluid's velocity rises & also the cavitation phenomenon increases. But the increase in steam due to the cavitation phenomenon works to reduce the efficiency of the pump & reduce the velocity of the outflow from the centrifugal pump.

1. Introduction

Because of the high pressures & speed of rotation of centrifugal pumps, it has become necessary to solve the problems of cavitation due to the great importance of pumps for all fields of industry & engineering in general. To study centrifugal pump performance under cavitating circumstances, a CFD approach is applied. For all flow coefficients, the fast decline in head coefficient at low cavitation numbers (breakdown) was represented. There were distinct performance patterns associated with off-design flow & blade cavitation [1]. Hydraulic machines are subjected to ever-increasingly stringent performance criteria. Cavitation in the suction chamber effectively dampens the water hammer caused by an abrupt shift in the location of the contact point. The volume of air becomes steadier at high rotating speeds, minimizing flow irregularity [2]. Vortices of varying strength were produced, & the velocity fields surrounding them were measured & compared to the equivalent fields derived by CFD calculations. The comparisons' results, as well as the difference between instantaneous & time-averaged velocity profiles, were detailed & debated [3]. Finding an ideal balance between pumping & producing performance is a significant design goal for cutting-edge reversible pump turbines. A suggested study outlines how sophisticated fluid dynamic (CFD) simulations might assist designers in evaluating their designs for hydraulic performance [4]. The Rayleigh-Plesset equation was used to compute the cavitating flow characteristic within a centrifugal pump, as well as bubble development & implosion. Six groups of hydraulic models were created to mimic & assess the model pump's internal two-phase flow under the identical conditions [5]. The computational fluid dynamics (CFD) simulations of the Schnerr–Sauer cavitation model with empirical coefficients are used to investigate the flow features of cavitation. The addition of a third phase to the cavitation model has a significant effect on the pump & NPSH cavitation's performance [6]. A novel "complete cavitation model" for forecasting the performance of engineering equipment under cavitating circumstances was recently created. As predicted, the results indicate cavitation zones on the leading-edge suction side of each machine. The water jet propulsion axial pump & an inducer from a LOX turbopump were simulated at various suction specie speeds [7]. A computational fluid dynamics (CFD) model of a positive displacement (PD) pump was built to simulate cavitation during the suction stroke. Three plunger speeds were simulated [8]. Cavitation flow can occur in the revolving runner-impeller or the stationary components of centrifugal pumps. Inception cavitation happens on the surface of the blade where the leading edge meets the tip. Lower NPSH values cause the cavitation zones to shift from the leading to the trailing edge [9]. Here, transient numerical computations for the flow field within a centrifugal pump were performed using CFD with varying numbers of impeller blades. Pressure fluctuations in both the time & frequency domains at the pump's impeller & volute were also analyzed [10]. Pump modeling using Computational Fluid Dynamics (CFD) has historically proven difficult & time consuming. Pump cavitation simulation has greatly improved in recent years. The purpose of this work [11] was to discuss a new generation CFD tool for pump cavitation modeling using an axial flow water pump as an example. Cavitation is a typical phenomenon that occurs during hydraulic turbomachine operation, lowering the performance & life of centrifugal pumps. The needed Net Positive Suction Head (NPSHr) has been determined using CFD simulations following the adoption of the cavitation model [12]. An article describes a novel NPSHr prediction method. The approach avoids conducting simulations under extreme cavitation conditions, resulting in faster convergence & simulation duration [13]. Research looked at how The No. of notches had an effect on the pressure distribution, void percent, & cavitation volume. area in an oil hydraulic pump. CFD findings are shown to be in good agreement with high-speed video camera data [14]. Cavitation instabilities were identified around the NPSH3 value at 70% of the ideal flow coefficient. For a wide variety of flow coefficients & NPSh values, CFD analysis revealed a good representation of the cavitation structures inside the pump & their movements [15].

Where in this research paper, a set of different pressures & rotational speeds were used to study their effect on cavitation through simulation with the CFD program.

2. Methodology

The part that forms the water shape of the centrifugal pump is completely designed by the SOLIDWORKS program that specializes in designing complex & precise geometric shapes as shown in the following figure:

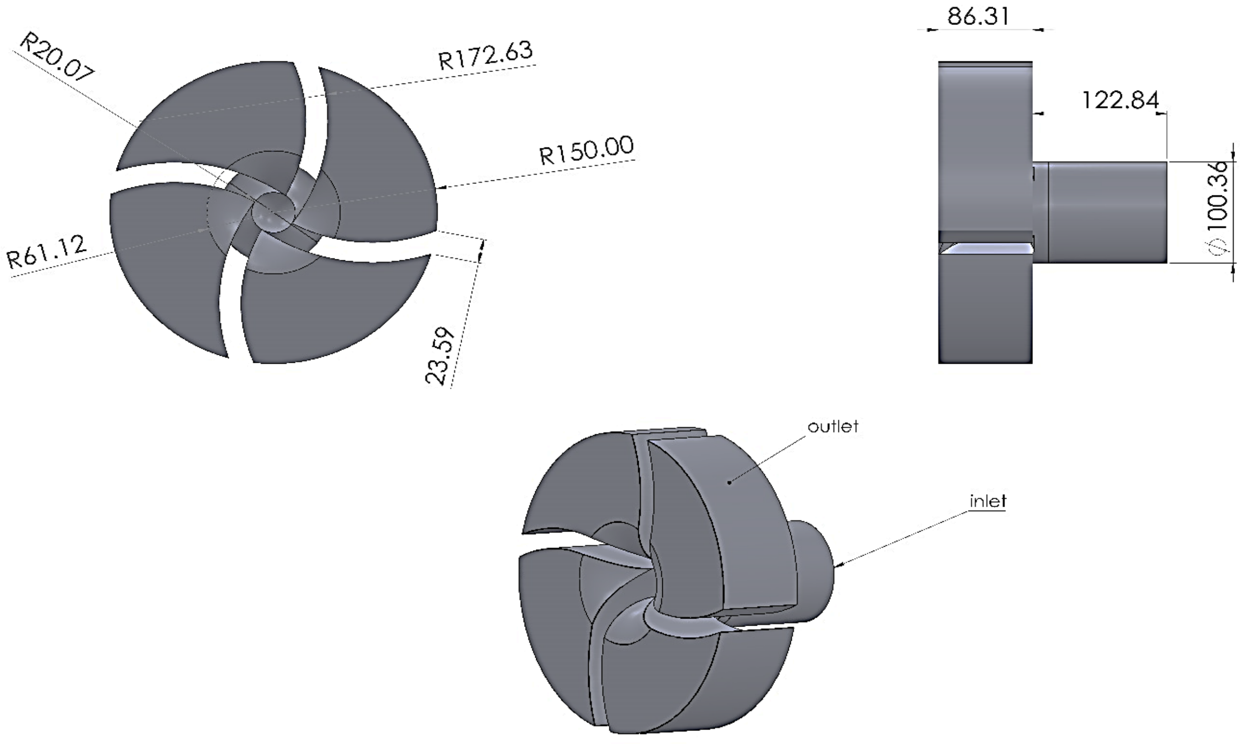

Figure (1): Geometry dimensions.

Where the ANSYS CFD program was used mainly in the simulation process, & in order for the simulation process to take place, a suitable mesh must be set to solve the governing equations in the CFD program, where the mesh number was changed in order to obtain a constant flow velocity with the change of the mesh as in the following table:

Table (1): Mesh Independency.

Case	Nodes	Elements	Max. velocity (m/s)
1	24800	103256	37.54
2	41237	214566	34.99
3	62032	340788	33.87
4	80150	405979	33.66

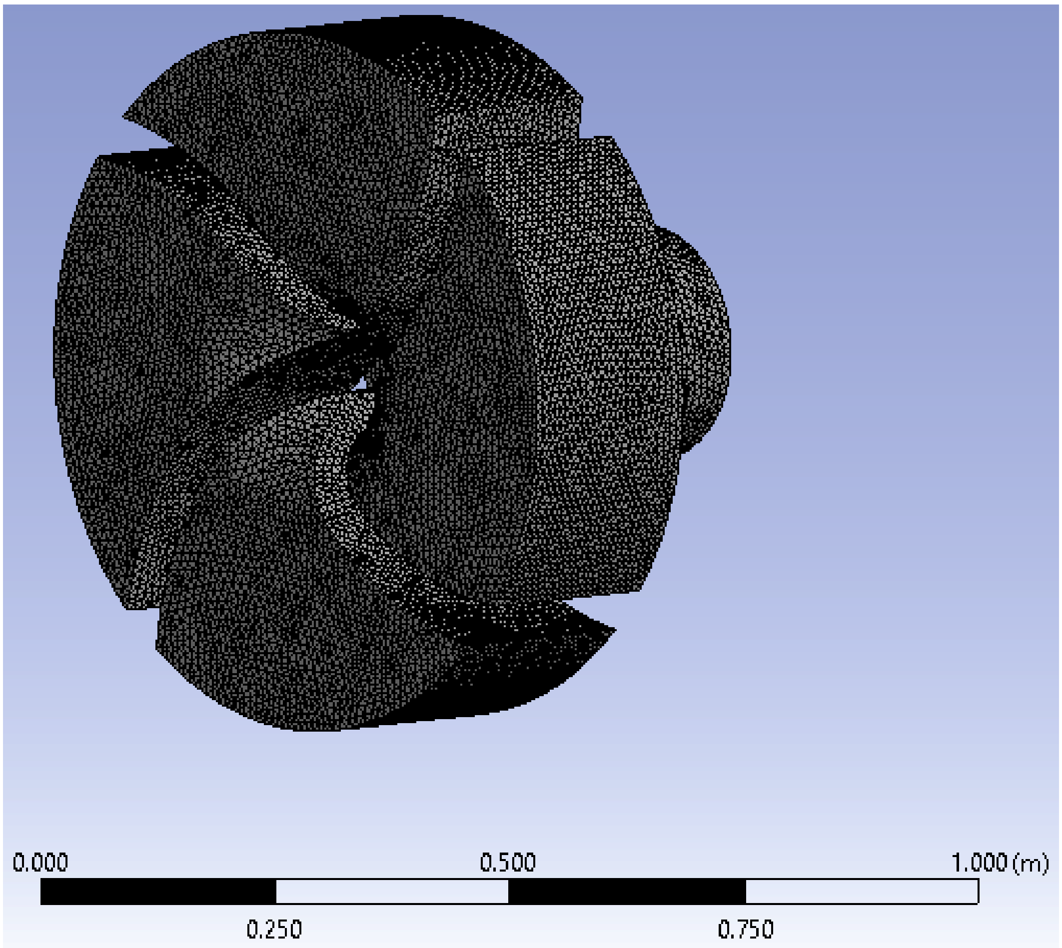

Figure (2): Geometry Mesh.

Where the settings were set in a way that suits the simulated situation, the viscosity model was set for the k-e equation & with the activation of a multiphase model due to the use of water in its fluid & vapor phases & a mass conversion activated using the cavitation model, & the physical properties of water & vapor were set, where a set of pressures was used in Entry area & different rotation speed for the whole model.

Table (2): Properties.

Properties	Unit	water/fluid	water/vapor
Density	kg/m^3	998.2	0.5542
Viscosity	kg/m.s	0.001003	0.0000134

3. Governing equations

A simple two-phase cavitation model employing the multiphase cavitation modeling technique consists of controlling the transport of mixtures (Mixture model) or phases (Eulerian multiphase) using standard viscous flow equations & a standard turbulence model (k-e model). The vapor transport equation governs the fluid-vapor mass transfer (evaporation & condensation) in cavitation:

$$\frac{\partial}{\partial t}(\alpha\rho_v) + \nabla \cdot \left(\alpha\rho_v\vec{V}_v\right) = R_e - R_c \qquad \ldots\ldots\ldots\ldots\ldots\ldots\ldots (1)$$

where

$v =$ vapor phase
$\alpha =$ vapor volume fraction
$\rho_v =$ vapor density
$\vec{V}_v =$ vapor phase velocity

$R_e, R_c =$ Source terms for mass transfer associated with the rise & collapse of vapor bubbles

The quantities R_e & R_c in Equation 1 Mass transport between the fluid & vapor phases is taken into consideration in cavitation. They are modeled in Ansys Fluent using the Rayleigh-Plesset equation, which is a term that refers to the formation of a single vapor bubble in a fluid.

In the majority of engineering applications, we assume that there are an enough number of nuclei for cavitation. to begin. As a result, the appropriate accounting of bubble expansion & collapse is our key concern. The extended Rayleigh-Plesset equation may be used to obtain the bubble dynamics in a fluid with no velocity slip between the fluid & the bubbles.

$$\Re_b \frac{D^2\Re_b}{Dt^2} + \frac{3}{2}\left(\frac{D\Re_b}{Dt}\right)^2 = \left(\frac{P_b - P}{\rho_l}\right) - \frac{4v_\ell}{\Re}\Re_b - \frac{2\sigma}{\rho_l \Re R_b} \qquad \ldots\ldots\ldots\ldots\ldots\ldots (2)$$

where,

$\Re_b =$ bubble radius
$\sigma =$ fluid surface tension coefficien
$\rho_l =$ fluid density
$v_l =$ fluid kinematic viscosity
$P_b =$ bubble surface pressure
$P =$ local far-field pressure

Equation 2 is simplified by omitting the second-order variables & the surface tension force.

$$\frac{D\Re_B}{Dt} = \sqrt{\frac{2}{3}\frac{P_b - P}{\rho_l}} \qquad \ldots\ldots\ldots\ldots\ldots\ldots\ldots\ldots (3)$$

This equation gives a physical method for incorporating cavitation model by including bubble dynamics. Additionally, it may be thought of as a vacuum propagation equation &, by extension, a mixture density equation.

Schnerr & Sauer use an approach similar to that used by Singhal et al. to derive the precise equation for net mass transfer from fluid to vapor. The vapor volume fraction equation has the following general form:

$$\frac{\partial}{\partial t}(\alpha\rho_v) + \nabla \cdot \left(\alpha\rho_v\vec{V}\right) = \frac{\rho_v\rho_l}{\rho}\frac{D\alpha}{Dt} \qquad \ldots\ldots\ldots\ldots\ldots\ldots (4)$$

The net mass source concept in this context is as follows:

$$R = \frac{\rho_v \rho_l}{\rho} \frac{d\alpha}{dt} \quad \text{……………………..} (5)$$

Schnerr & Sauer, in contrast to Zwart-Gerber-Belamri & Singhal et al., use the following equation to calculate the proportion of vapor volume in a volume of fluid:

$$\alpha = \frac{n_b \frac{4}{3} \pi \Re_B^3}{1 + n_b \frac{4}{3} \pi \Re_B^3} \quad \text{………………….} (6)$$

Using a method similar to Singhal et al., they arrived at the following equation:

$$R = \frac{\rho_v \rho_l}{\rho} \alpha(1-\alpha) \frac{3}{\Re_B^2} \sqrt{\frac{2}{3} \frac{(P_v - P)}{\rho_l}} \quad \text{……………………..} (7)$$

$$\Re_B = \left(\frac{\alpha}{1-\alpha} \frac{3}{4\pi} \frac{1}{n} \right)^{\frac{1}{3}} \quad \text{……………………..} (8)$$

where,

$R =$ mass transfer rate
$\Re_B =$ bubble radius

When Equation 7 is compared to Equation 4, Unlike the two preceding models, it is evident that the mass transfer rate in the Schnerr & Sauer model is proportional to $\alpha_v(1-\alpha_v)$. Moreover, the function $f(\alpha_v, \rho_v, \rho_l) = \frac{\rho_v \rho_l}{\rho} \alpha(1-\alpha)$ has the unusual trait of approaching zero when $\alpha = 0$ & $\alpha = 1$, & reaching the maximum in between. The sole parameter that must be calculated in this model is the number of spherical bubbles per volume of fluid. The bubble number density would be constant if no bubbles were formed or destroyed. As a result, The initial circumstances for the volume percentage of the nucleation site & the radius of the equilibrium bubble would be sufficient to calculate the bubble number density (n) from Equation 6 & the phase transition from Equation 7.

Equation 7 is employed to simulate the condensation process, as it is in the other two models. The model's final shape is as follows:

When $P_v \geq P$,

$$R_e = F_{\text{vap}} \frac{\rho_v \rho_l}{\rho} \alpha(1-\alpha) \frac{3}{\Re_B} \sqrt{\frac{2}{3} \frac{(P_v - P)}{\rho_l}} \quad \text{………………….} (9)$$

When $P_v \leq P$,

$$R_c = F_{\text{cond}} \frac{\rho_v \rho_l}{\rho} \alpha(1-\alpha) \frac{3}{\Re_B} \sqrt{\frac{2}{3} \frac{(P - P_v)}{\rho_l}} \quad \text{……………………} (10)$$

where F_{vap} & F_{cond} are the empirical evaporation & condensation coefficients with default values of 1 & 0.2, respectively. These coefficients can be changed using the expert text command option, as detailed in Mass Transfer Mechanisms in the Fluent User's Guide.

4. Results & discussion

4.1 The effect of rotational speed on cavitation

Where the pressure of 1bar was used in this case & the results were verified by the flow velocity of the fluid & the amount of vapor produced by the cavitation phenomenon.

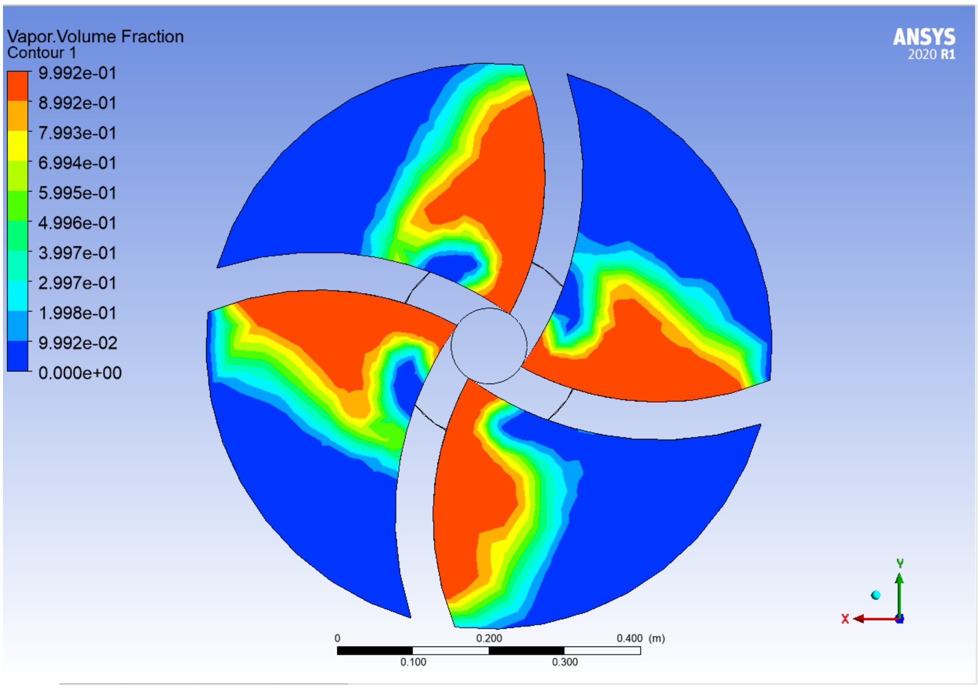

Vapor.Volume Fraction
Contour 1
9.992e-01
8.992e-01
7.993e-01
6.994e-01
5.995e-01
4.996e-01
3.997e-01
2.997e-01
1.998e-01
9.992e-02
0.000e+00
ANSYS
2020 R1
0
0.200
0.400 (m)
0.100
0.300
Y
X

(a)

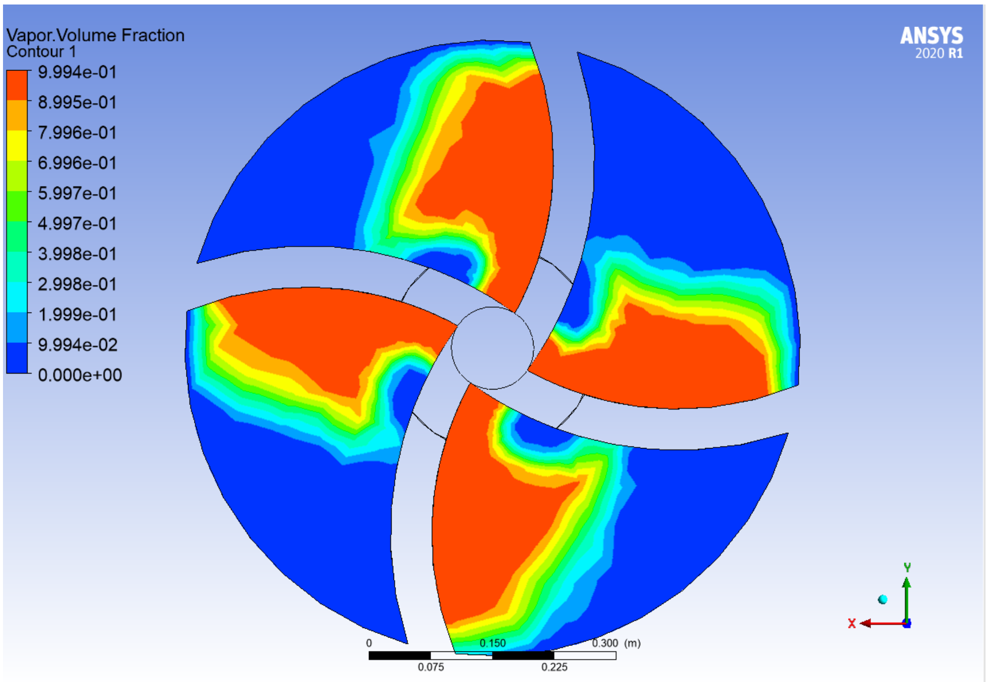

Vapor.Volume Fraction
Contour 1
9.994e-01
8.995e-01
7.996e-01
6.996e-01
5.997e-01
4.997e-01
3.998e-01
2.998e-01
1.999e-01
9.994e-02
0.000e+00
ANSYS
2020 R1
0
0.150
0.300 (m)
0.075
0.225
Y
X

(b)

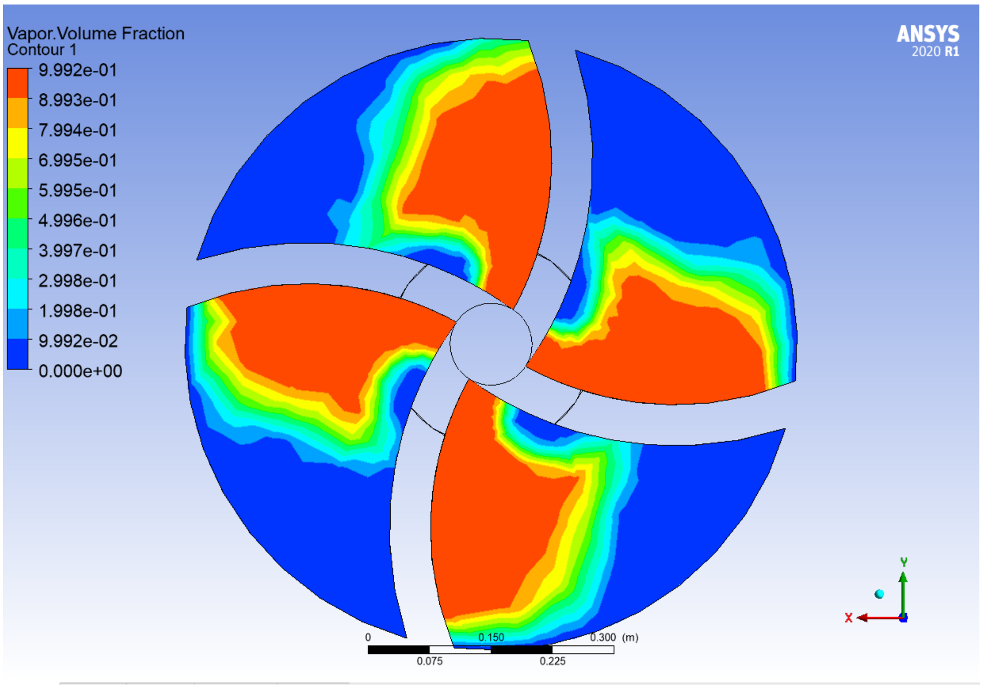

(c)

Figure (3): Vapor Volume Fraction (a) 800 rpm, (b) 1000 rpm, (c) 1200 rpm.

Through the previous figures for volume fraction of steam produced by the cavitation phenomenon, we note that with the increase in the rotational speed, the efficiency of the cavitation phenomenon increases & becomes significantly affecting the efficiency of the centrifugal pump, as the largest amount of steam produced was at 1200 rpm.

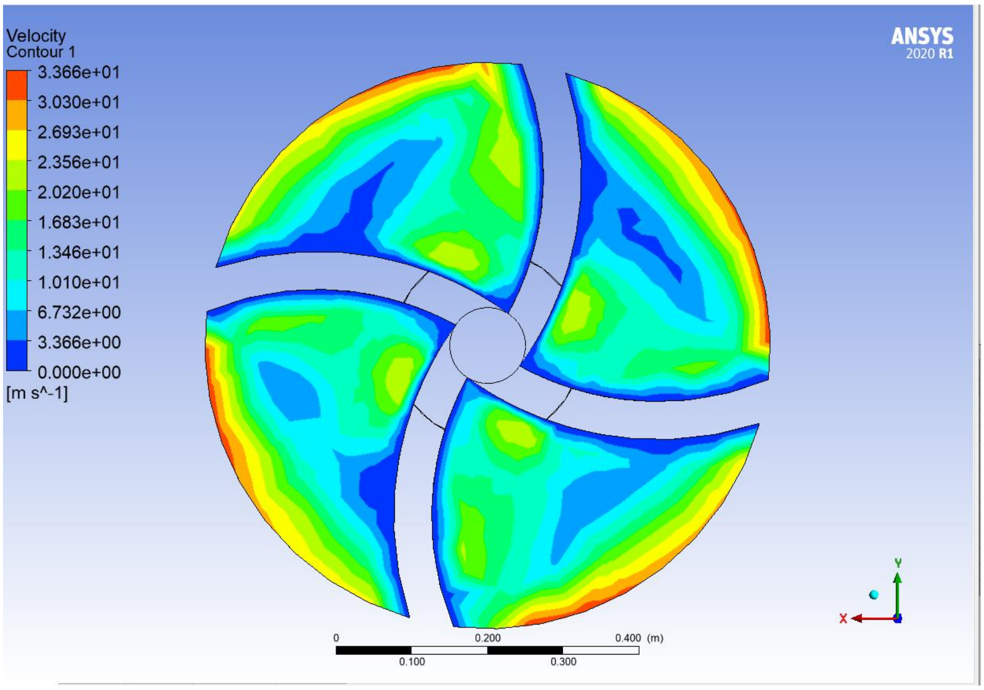

(a)

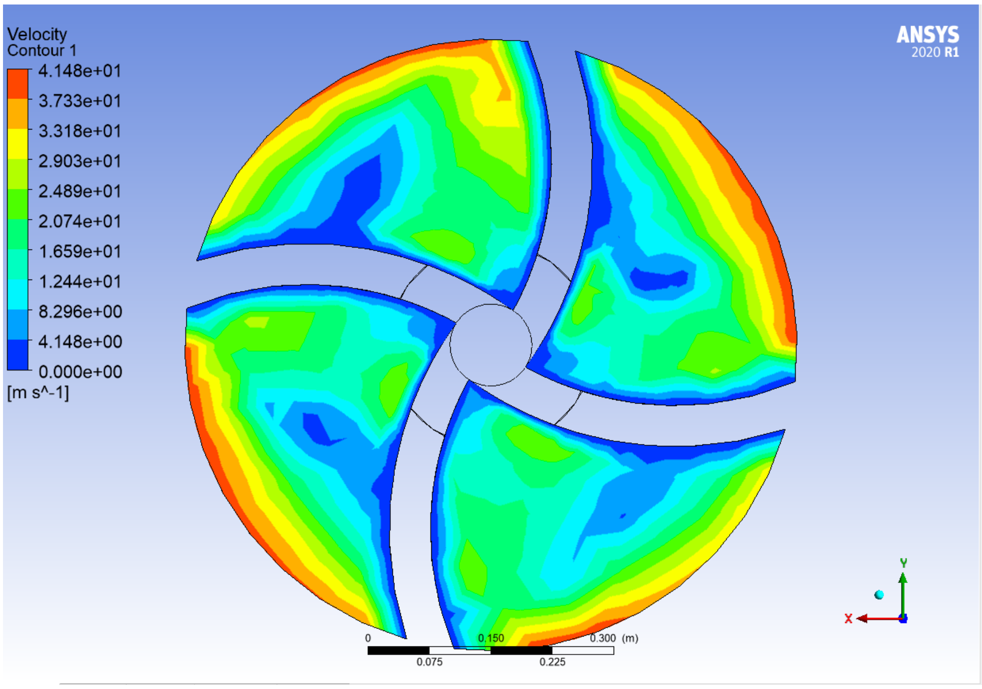

(b)

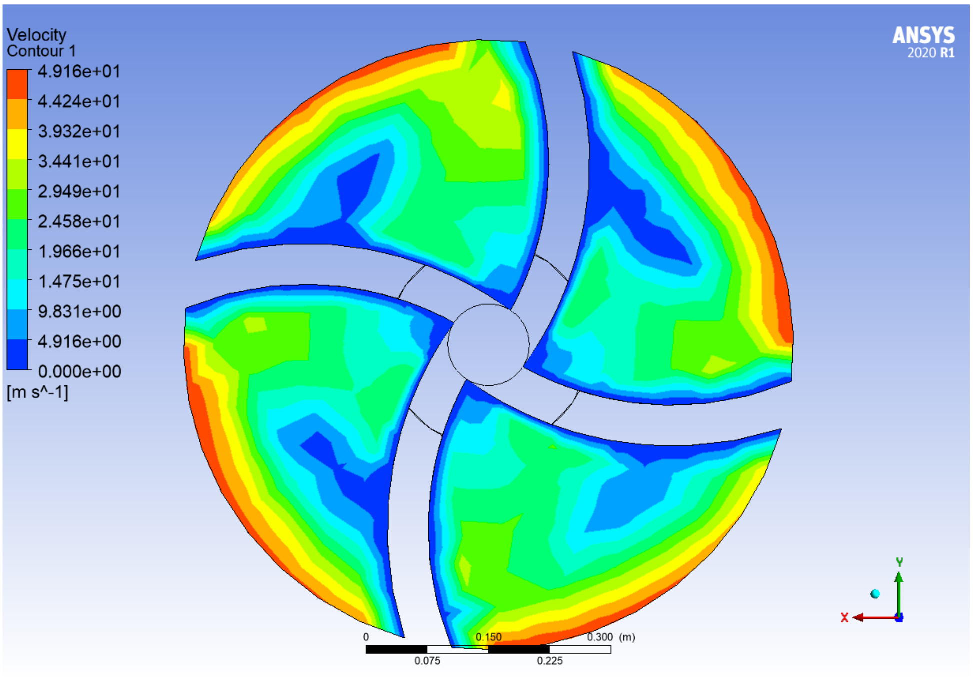

(c)

Figure (4): Velocity (a) 800 rpm, (b) 1000 rpm, (c) 1200 rpm.

With the increase in the rotational speed, the flow rate of the water increases, as the fluid velocity is faster when rotating at high speeds, as we notice this thing through the previous figures, where the velocity of water flow reached 49.16 m/s at a rotational speed of 1200 rpm.

4.2 The effect of the increase in pressure on the cavitation phenomenon

One of the most important reasons that lead to the occurrence of cavitation is the increase in pressure inside the centrifugal pump, where five pressures were taken that were authorized for the pump to understand the occurrence of the phenomenon of cavitation.

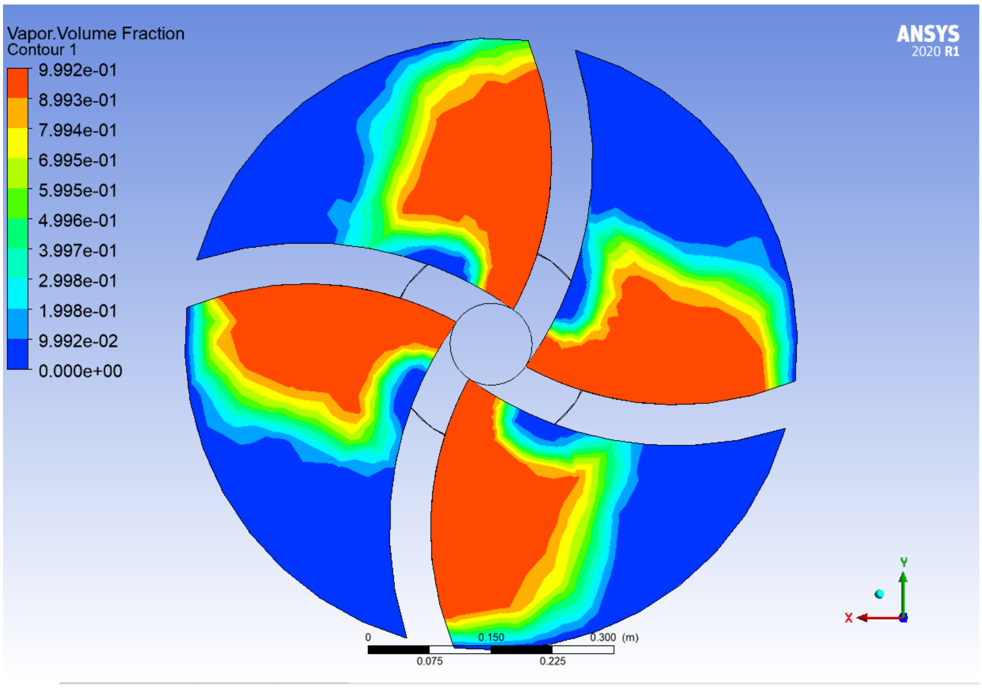
Vapor.Volume Fraction
Contour 1
9.992e-01
8.993e-01
7.994e-01
6.995e-01
5.995e-01
4.996e-01
3.997e-01
2.998e-01
1.998e-01
9.992e-02
0.000e+00
ANSYS
2020 R1
0
0.150
0.300 (m)
0.075
0.225

(a)

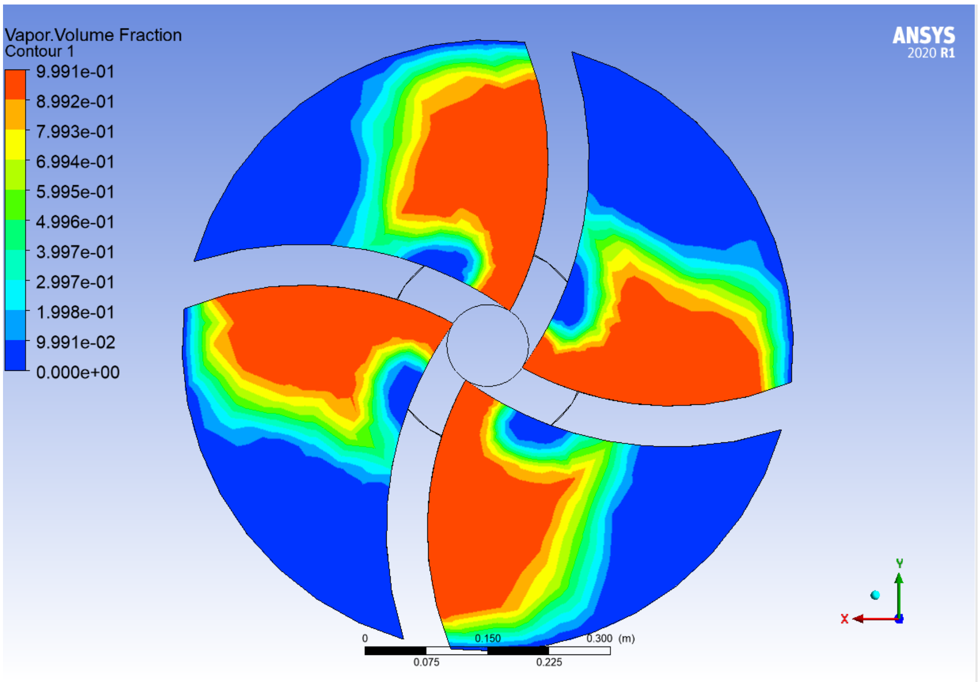
Vapor.Volume Fraction
Contour 1
9.991e-01
8.992e-01
7.993e-01
6.994e-01
5.995e-01
4.996e-01
3.997e-01
2.997e-01
1.998e-01
9.991e-02
0.000e+00
ANSYS
2020 R1
0
0.150
0.300 (m)
0.075
0.225

(b)

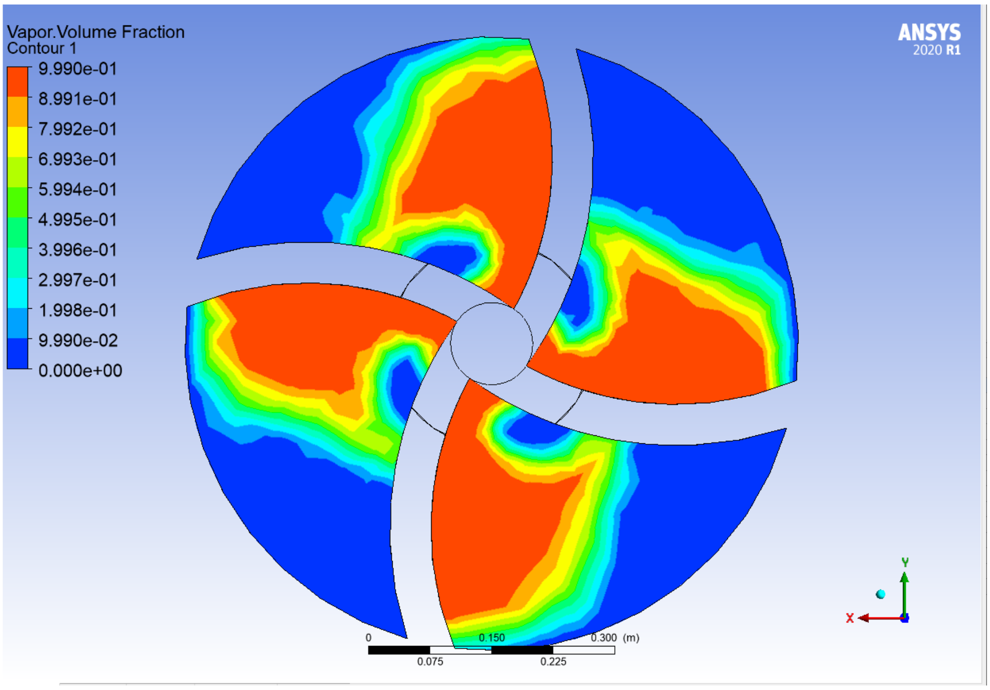

Vapor.Volume Fraction
Contour 1
9.990e-01
8.991e-01
7.992e-01
6.993e-01
5.994e-01
4.995e-01
3.996e-01
2.997e-01
1.998e-01
9.990e-02
0.000e+00
ANSYS
2020 R1
0
0.150
0.300 (m)
0.075
0.225

(c)

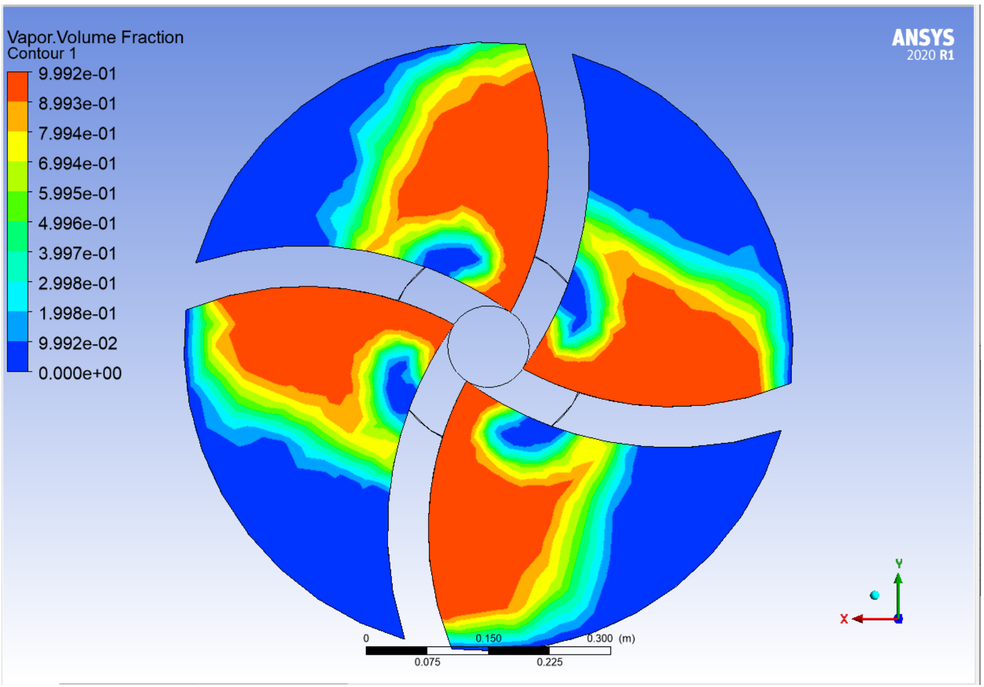

Vapor.Volume Fraction
Contour 1
9.992e-01
8.993e-01
7.994e-01
6.994e-01
5.995e-01
4.996e-01
3.997e-01
2.998e-01
1.998e-01
9.992e-02
0.000e+00
ANSYS
2020 R1
0
0.150
0.300 (m)
0.075
0.225

(d)

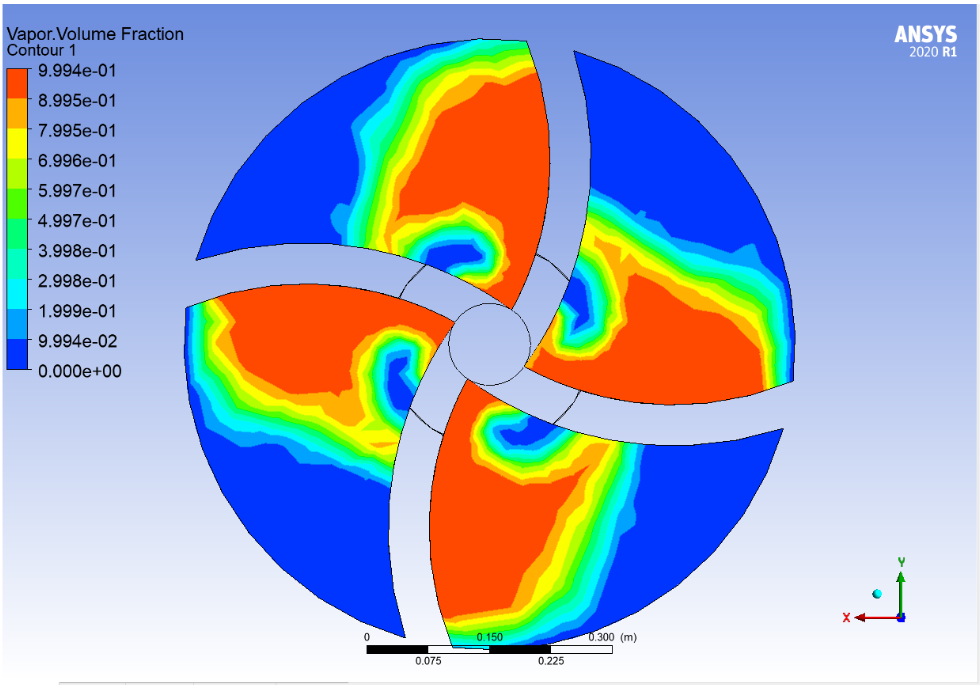

(e)

Figure (5): Vapor Volume Fraction (a) 1 bar, (b) 2 bar, (c) 3 bar, (d) 4 bar, (e) 5 bar.

We also note through the previous forms of vapor values & their distribution as a result of the cavitation phenomenon. We can understand well the effect of pressure on the phenomenon of cavitation, as the amount of vapor resulting from the phenomenon of cavitation at pressure is 5 bar.

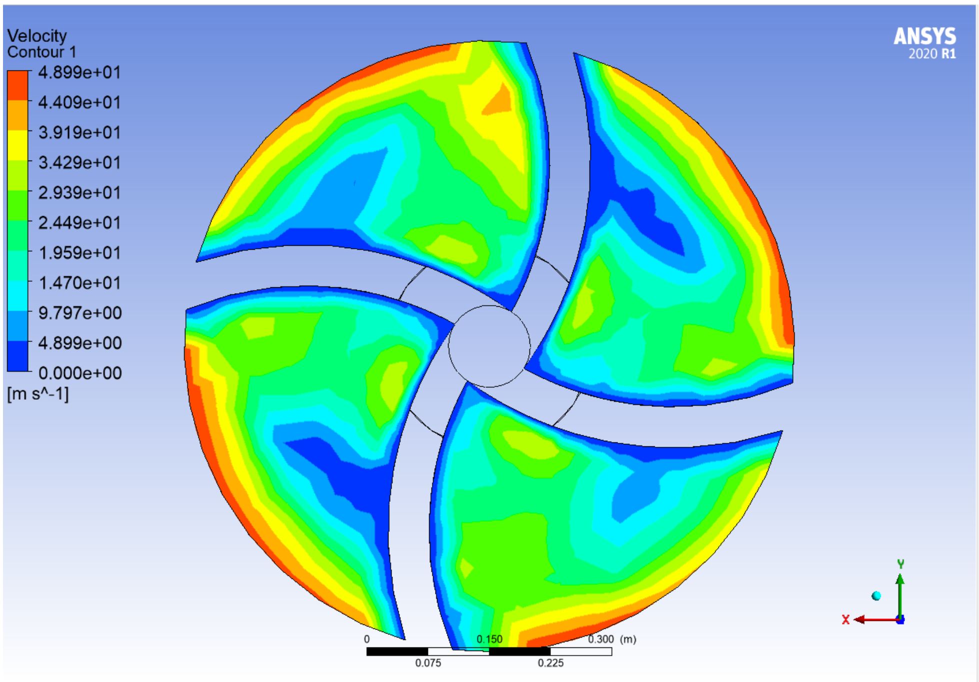

(a)

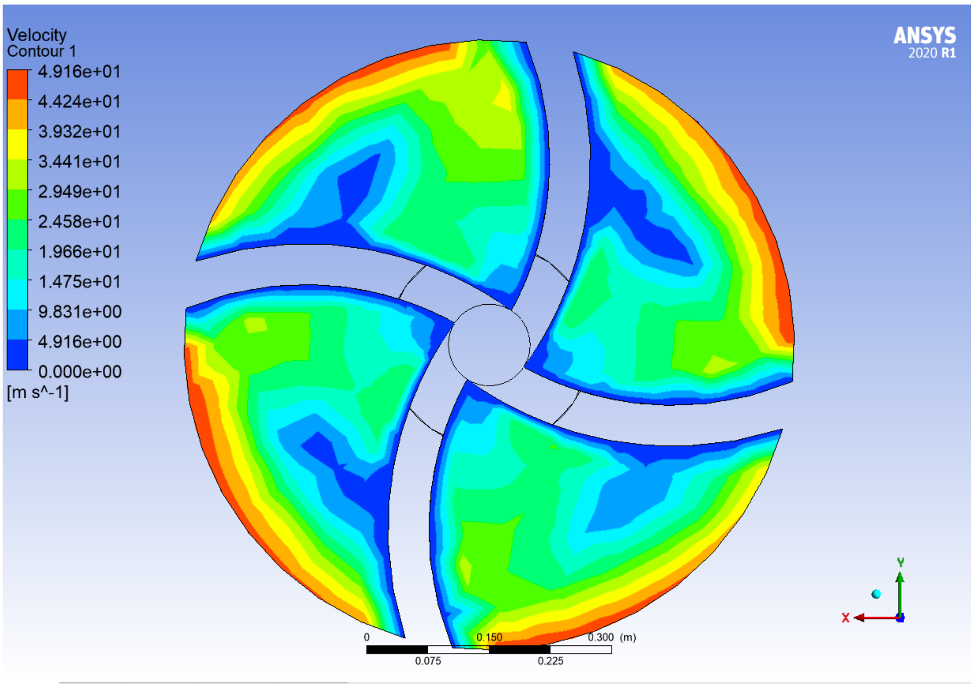

Velocity
Contour 1
4.916e+01
4.424e+01
3.932e+01
3.441e+01
2.949e+01
2.458e+01
1.966e+01
1.475e+01
9.831e+00
4.916e+00
0.000e+00
[m s^-1]
ANSYS
2020 R1
0
0.150
0.300 (m)
0.075
0.225

(b)

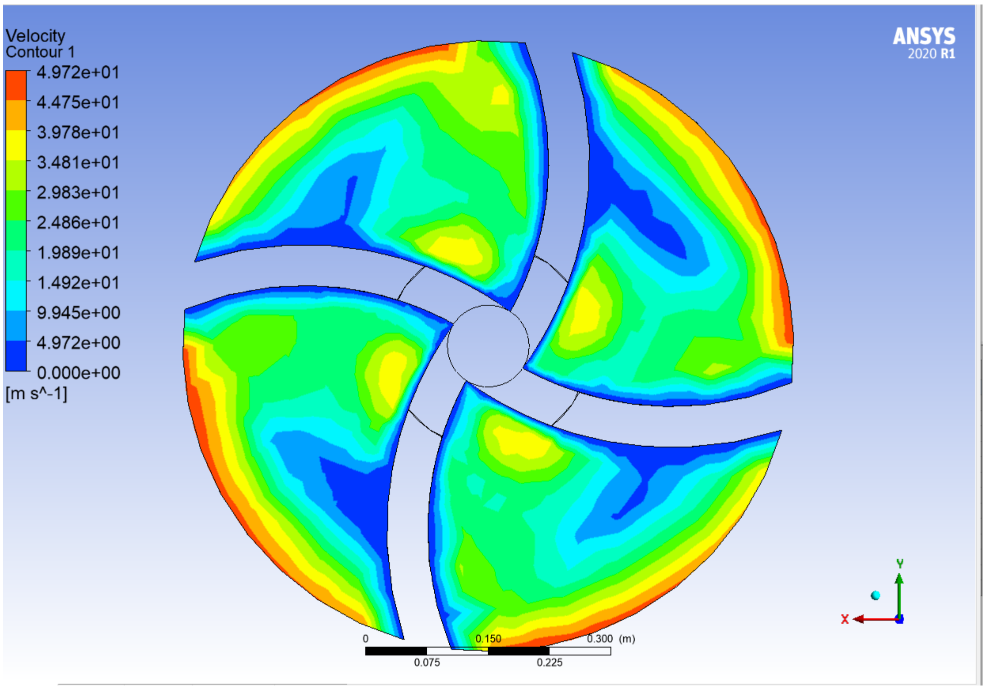

Velocity
Contour 1
4.972e+01
4.475e+01
3.978e+01
3.481e+01
2.983e+01
2.486e+01
1.989e+01
1.492e+01
9.945e+00
4.972e+00
0.000e+00
[m s^-1]
ANSYS
2020 R1
0
0.150
0.300 (m)
0.075
0.225

(c)

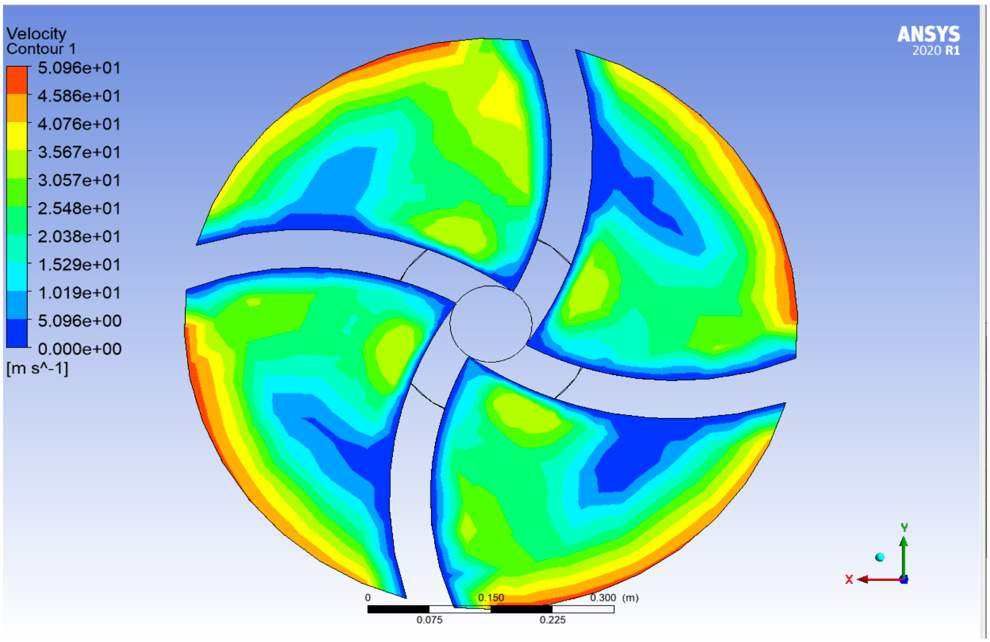

(d)

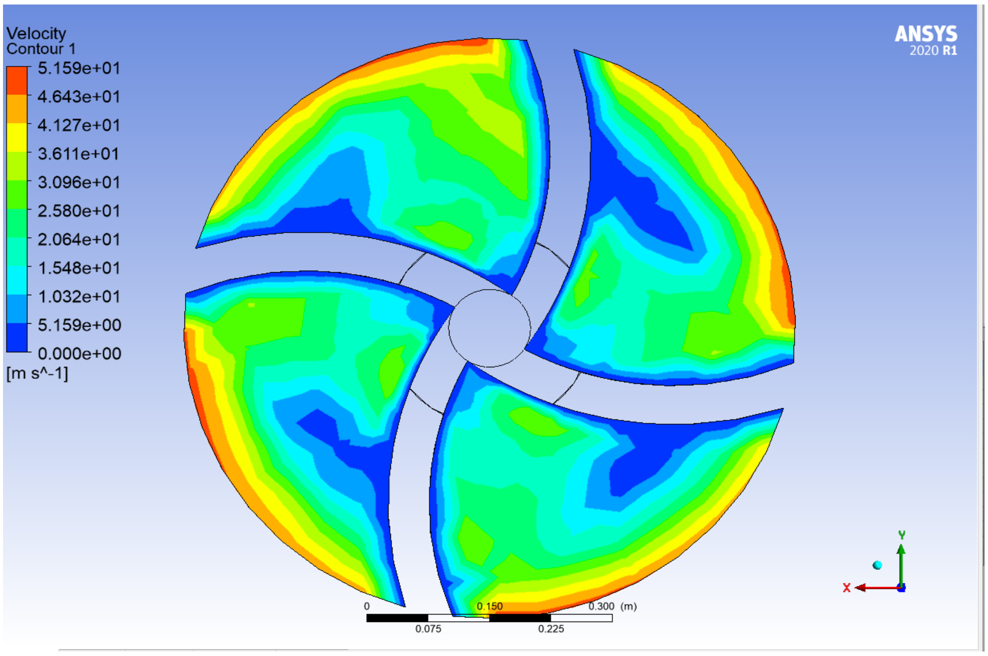

(e)

Figure (6): Velocity. (a) 1 bar, (b) 2 bar, (c) 3 bar, (d) 4 bar, (e) 5 bar.

The increase in the pressure values has a significant effect on the fluid flow velocity, as it was noted through the previous figures for the fluid flow velocity that the largest pressure that was prepared gives the largest flow velocity of the fluid inside the centrifugal pump, as the pressure 5 bar gave a flow velocity of 51.59 m/s.

5. Conclusions

In this research paper, the effect of the centrifugal pump rotation speed & the supplied pressure of the pump & its effect on the cavitation phenomenon was studied, as it was observed through the results extracted as follows:

1. The increase in the rotational speed of the pump increases the fluid flow velocity & thus increases the internal pressure of the centrifugal pump, as this increase greatly affects the cavitation structures that reduce the efficiency of the pump, as it was found that the largest value that can affect is at 1200 rpm.
2. The main condition for the occurrence of the cavitation phenomenon is the noticeable increase in the pressure produced inside the pump. When preparing the centrifugal pump, we notice the increase in the flow velocity of the fluid & the amount of steam produced by the cavitation phenomenon, which in turn reduces the efficiency of the centrifugal pump, as it was found that the largest pressure 5bar is the most effective pressure in a way Great for cavitation.

References

1. Medvitz, Richard B.; Kunz, Robert F.; Boger, David A.; Lindau, Jules W.; Yocum, Adam M.; Pauley, Laura L. (2002). Performance Analysis of Cavitating Flow in Centrifugal Pumps Using Multiphase CFD. Journal of Fluids Engineering, 124(2), 377–. doi:10.1115/1.1457453.
2. Del Campo, D.; Castilla, R.; Raush, G. A.; Gamez Montero, P. J.; Codina, E. (2012). Numerical Analysis of External Gear Pumps Including Cavitation. Journal of Fluids Engineering, 134(8), 081105–. doi:10.1115/1.4007106.
3. Anciger, D; Jung, A; Aschenbrenner, T (2010). Prediction of rotating stall & cavitation inception in pump turbines. IOP Conference Series: Earth & Environmental Science, 12(), 012013–. doi:10.1088/1755-1315/12/1/012013.
4. Xie, S F; Wang, Y; Liu, Z C; Zhu, Z T; Ning, C; Zhao, L F (2015). Optimization of centrifugal pump cavitation performance based on CFD. IOP Conference Series: Materials Science & Engineering, 72(3), 032023–. doi:10.1088/1757-899X/72/3/032023.
5. Lomakin, V; Bibik, O (2019). Numerical prediction of the gas content effect on the cavitation characteristics of the pump using the simplified Rayleigh-Plesset equation. IOP Conference Series: Materials Science & Engineering, 492(), 012037–. doi:10.1088/1757-899X/492/1/012037.
6. Athavale, Mahesh M.; Li, H. Y.; Jiang, Yu; Singhal, Ashok K. (2002). Application of the Full Cavitation Model to Pumps & Inducers. International Journal of Rotating Machinery, 8(1), 45–56. doi:10.1155/s1023621x02000052.
7. Iannetti, Aldo; Stickland, Matthew T.; Dempster, William M. (2016). A CFD & experimental study on cavitation in positive displacement pumps: Benefits & drawbacks of the 'full' cavitation model. Engineering Applications of Computational Fluid Mechanics, 10(1), 57–71. doi:10.1080/19942060.2015.1110535.
8. Ding, H.; Visser, F. C.; Jiang, Y.; Furmanczyk, M. (2011). Demonstration & Validation of a 3D CFD Simulation Tool Predicting Pump Performance & Cavitation for Industrial Applications. Journal of Fluids Engineering, 133(1), 011101–. doi:10.1115/1.4003196.
9. Jeanty, Freddy; De Andrade, Jesús; Asuaje, Miguel; Kenyery, Frank; Vásquez, Auristela; Aguillón, Orlando; Tremante, Andrés (2009). [ASME ASME 2009 Fluids Engineering Division Summer Meeting - Vail, Colorado, USA (August 2–6, 2009)] Volume 1: Symposia, Parts A, B & C - Numerical Simulation of Cavitation Phenomena in a Centrifugal Pump, 331–338. doi:10.1115/fedsm2009-78303.
10. Ding, H.; Visser, F. C.; Jiang, Y. (2012). [ASME ASME 2012 Fluids Engineering Division Summer Meeting collocated with the ASME 2012 Heat Transfer Summer Conference & the ASME 2012 10th International Conference on Nanochannels, Microchannels, & Minichannels - Rio Grande, Puerto Rico, USA (Sunday 8 July 2012)] Volume 1: Symposia, Parts A & B - A Practical Approach to Speed Up NPSHr Prediction of Centrifugal Pumps Using CFD Cavitation Model. , (), 505–. doi:10.1115/fedsm2012-72282.
11. Tsukiji, Tetsuhiro; Nakayama, Kensuke; Saito, Keiji; Yakabe, Shinji (2011). [IEEE 2011 International Conference on Fluid Power & Mechatronics (FPM) - Beijing, China (2011.08.17-2011.08.20)] Proceedings of 2011 International Conference on Fluid Power & Mechatronics - Study on the cavitating flow in an oil hydraulic pump, (), 253–258. doi:10.1109/fpm.2011.6045768.
12. Sedlar, Milan; Sputa, Oldrich; Komarek, Martin (2012). CFD Analysis of Cavitation Phenomena in Mixed-Flow Pump. International Journal of Fluid Machinery & Systems, 5(1), 18–29. doi:10.5293/IJFMS.2012.5.1.018.
13. Tsutsumi, Keisuke; Watanabe, Satoshi; Tsuda, Shin-ichi; Yamaguchi, Takeshi (2016). Cavitation simulation of automotive torque converter using a homogeneous cavitation model. European Journal of Mechanics - B/Fluids, (), S0997754616303715–. doi:10.1016/j.euromechflu.2016.09.001.
14. Shah, S.R.; Jain, S.V.; Patel, R.N.; Lakhera, V.J. (2013). CFD for Centrifugal Pumps: A Review of the State-of-the-Art. Procedia Engineering, 51(), 715–720. doi:10.1016/j.proeng.2013.01.102.
15. Alexander Steinmann; Hendrik Wurm; Alfred Otto (2010). Numerical & experimental investigations of the unsteady cavitating flow in a vortex pump, 22(5-supp-S1), 324–329. doi:10.1016/s1001-6058(09)60213-4.